

## Trafficking mechanisms underlying $\text{Na}_v$ channel subcellular localization in neurons

Laura Solé<sup>a,b</sup> and Michael M. Tamkun<sup>a,b,c</sup>

<sup>a</sup>Molecular, Cellular and Integrative Neurosciences Graduate Program, Colorado State University, Fort Collins, CO, USA; <sup>b</sup>Department of Biomedical Sciences, Colorado State University, Fort Collins, CO, USA; <sup>c</sup>Department of Biochemistry and Molecular Biology, Colorado State University, Fort Collins, CO, USA

### ABSTRACT

Voltage gated sodium channels ( $\text{Na}_v$ ) play a crucial role in action potential initiation and propagation. Although the discovery of  $\text{Na}_v$  channels dates back more than 65 years, and great advances in understanding their localization, biophysical properties, and links to disease have been made, there are still many questions to be answered regarding the cellular and molecular mechanisms involved in  $\text{Na}_v$  channel trafficking, localization and regulation. This review summarizes the different trafficking mechanisms underlying the polarized  $\text{Na}_v$  channel localization in neurons, with an emphasis on the axon initial segment (AIS), as well as discussing the latest advances regarding how neurons regulate their excitability by modifying AIS length and location. The importance of  $\text{Na}_v$  channel localization is emphasized by the relationship between mutations, impaired trafficking and disease. While this review focuses on  $\text{Na}_v1.6$ , other  $\text{Na}_v$  isoforms are also discussed.

### ARTICLE HISTORY

Received 25 October 2019  
Revised xx xxx xxxx  
Accepted 13 November 2019

### KEYWORDS

Voltage-gated sodium channel;  $\text{Nav}1.6$ ; trafficking; axon initial segment; plasticity; ion channel localization; channelopathies

### Introduction

Voltage-gated sodium channels ( $\text{Na}_v$ ) are essential for the initiation and propagation of most action potentials (APs). There are 9 isoforms of the pore-forming  $\alpha$  subunits ( $\text{Na}_v1.1$ – $9$ ).  $\text{Na}_v1.1$ ,  $\text{Na}_v1.2$ ,  $\text{Na}_v1.3$  and  $\text{Na}_v1.6$  are primarily expressed in the central nervous system (CNS), while  $\text{Na}_v1.7$ ,  $\text{Na}_v1.8$  and  $\text{Na}_v1.9$  are predominant in the peripheral nervous system.  $\text{Na}_v1.4$  and  $\text{Na}_v1.5$  are mostly expressed in skeletal muscle and in heart, respectively [1,2]. Each functional  $\text{Na}_v$  is formed by a multimer of a  $\alpha$  subunit with 4 homologous domains (each with 6 transmembrane domains) and at least one auxiliary  $\beta$  subunit. There are 4 different  $\beta$  subunits ( $\beta1$ – $4$ ), all of them being single-span transmembrane proteins with an extracellular N-terminus. While  $\beta1$  and  $\beta3$  associate non-covalently with the  $\alpha$  subunit through their N- and C-terminal domains,  $\beta2$  and  $\beta4$  associate through a disulfide link with a cysteine within their N-terminal domain. Association with  $\beta$  subunits can affect  $\text{Na}_v$  channel function, location and trafficking [3].

The first identification of protein representing a  $\text{Na}_v$  channel involved the purification of tetrodotoxin (TTX) binding activity from the electric eel [4], which occurred almost 30 years after the classic Hodgkin and Huxley studies [5–7], as illustrated by the time line in Figure 1. This work was soon followed by studies done in the Catterall lab characterizing the rat brain  $\text{Na}_v$  protein [8–10] and establishing the concentration of  $\text{Na}_v$  channels at the axon initial segment (AIS) [11]. The cloning of the first  $\text{Na}_v$  channel from the electric eel by the Numa group [12] was followed quite rapidly by the identification of the first three mammalian  $\text{Na}_v$  isoforms [13,14]. Numerous structure function studies then dissected the gating and ion permeation mechanisms [15–21] and specific  $\text{Na}_v$  mutations were linked to human disease [22–24]. Progress in high resolution structure determination [25–27] added a physical context to much of the site-directed mutagenesis work that had occurred over the previous 20 years. Recent progress in  $\text{Na}_v$  channel biology focuses on the mechanisms underlying channel trafficking and localization and how localization determines

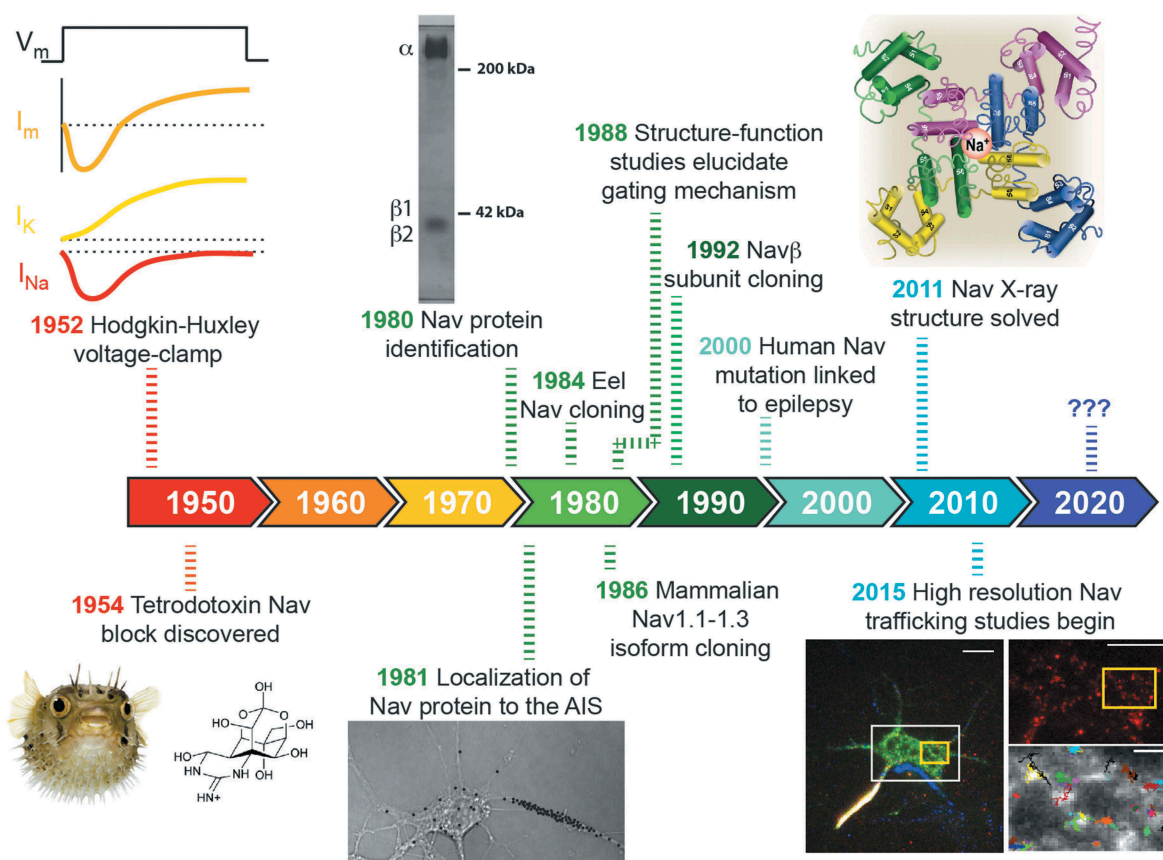


**Figure 1. Seventy years of  $\text{Na}_v$  channel history: From the squid giant axon to single molecule tracking.** The pufferfish, TTX and crystal structure images are used with permission from ref. 2 (<https://doi.10.1021/jm501981g>; Further permissions related to the excerpted material should be directed to the American Chemical Society). The SDS gel, autoradiography, and single molecule tracking images have not been published previously but relate to refs. 9, 11, and 56, respectively.

function [28,29], for proper nerve function requires the precise targeting of  $\text{Na}_v$  isoforms to distinct subcellular domains. While this review will mainly focus on the localization and trafficking of  $\text{Na}_v1.6$ , other  $\text{Na}_v$  channel isoforms will be discussed when appropriate.

### Discovery of $\text{Na}_v1.6$

$\text{Na}_v1.6$ , encoded by the *SCN8A* gene, had several names during the early years of cloning, such as *Rat6*, *NaCh6*, *Scn8a*, *PN4* and *CerIII*.  $\text{Na}_v1.6$  was first described almost simultaneously by two different labs in 1995, from two different species. Schaller et al. were the first to report the full sequence of the rat  $\text{Na}_v1.6$ , and detected its expression in brain by RT-PCR [30]. These investigators were surprised that, while  $\text{Na}_v1.6$  mRNA was one of the most abundant  $\text{Na}_v$  channel transcripts in the nervous system, it had not been cloned earlier (the mammalian  $\text{Na}_v1.1-1.3$

channels were first cloned in the mid-1980s [12,31]). They also demonstrated that it was expressed both in neurons and glia, with a broad distribution in CNS that was distinct from previously reported  $\text{Na}_v$  channels. For example, they found  $\text{Na}_v1.6$  in hippocampal pyramidal and granule cells, motor neurons of the spinal cord and brain stem, axons in the retina, and dendrites of cerebral cortical pyramidal cells. In parallel, Burgess et al., isolated a mouse  $\text{Na}_v$  channel gene, *Scn8a*, which was highly expressed in brain and spinal cord but not in skeletal muscle or heart, and encoded a predicted protein of 1,732 amino acids [32]. Interestingly, *Scn8a* was located in the flanking region of a transgene-induced allele of *med* (a mouse neurological mutant with motor endplate disease). This phenotype is characterized by early onset progressive paralysis of the hind limbs, severe muscle atrophy, degeneration of Purkinje cells and juvenile lethality. Later, Vega-Saenz et al., in 1997, identified expression of rat  $\text{Na}_v1.6$  by single-cell RT-PCR in cerebellum and

cerebellar Purkinje cells [33]. In agreement with Schaller et al., rat  $Na_v1.6$  mRNA, as detected by in situ hybridization, was found in many neuronal populations of the CNS, being a channel highly expressed in the brain and spinal cord. Furthermore,  $Na_v1.6$  was proposed to be responsible for the persistent and resurgent currents observed in Purkinje cells, since these currents were decreased in cultures of *Scn8a* null mice [34].  $Na_v1.6$  was also characterized as one of the major contributors to sodium current in mouse post-natal motor neurons [35]. The first functional characterization of mouse  $Na_v1.6$  was performed by Smith et al. in *Xenopus* oocytes, where they observed that  $Na_v1.6$  currents inactivated faster than other  $Na_v$  channel isoforms and presented a unique persistent current, which they concluded was responsible for distinct sodium conductances necessary for the repetitive firing of AP in Purkinje neurons [36].  $Na_v1.6$  protein was first described as concentrating at Nodes of Ranvier [37–39], but was later detected in axon initial segments of Purkinje neurons [40] and cerebellar granule cells [41], and in dendrites of pyramidal cells of the cortex, hippocampus and cerebellum [42].  $Na_v1.6$  was also expressed at lower levels in the somato-dendritic compartment [43,44] where it is likely responsible for the generation of dendritic action potentials [45].

### ***Na<sub>v</sub>1.6 and disease***

Mutations in mouse  $Na_v1.6$  have been associated with ataxia, muscle weakness, tremor, dystonia and juvenile lethality [32,46,47], and conditional deletion of *Scn8a* in mouse cerebellar neurons resulted in mild ataxia [48]. However, it was not until the mid-2000s that the first human mutation in *SCN8A* was found in a patient with mental retardation, ataxia and cerebellar atrophy [49]. Later, in 2012, mutations in *SCN8A* were associated for the first time with early infantile epileptic encephalopathy (EIEE13, OMIM #614558). The first epileptic-related *SCN8A de novo* mutation described was in a 15-year-old female who had severe epileptic encephalopathy, some features of autism, intellectual disability, ataxia and died of SUDEP (sudden unexplained death in epilepsy) [50]. Subsequently, and thanks primarily to advances in genome sequencing technology, the number of clinical cases associated with  $Na_v1.6$

has increased significantly, with more than 140 patients now diagnosed with *SCN8A* mutations [51]. Mutations in *SCN8A* are also associated with benign familial infantile seizures-5 (BFIS5, OMIM #617080) [52–54]. In a meta analysis of epilepsy genetics research over the past decade, from 5185 papers published from 2009 to 2018, 4% of the “occurrences” related with epilepsy corresponded to *SCN8A* mutations [55].

### ***Subcellular localization of Na<sub>v</sub>1.6***

As mentioned earlier,  $Na_v1.6$  is highly concentrated at the AIS and Nodes of Ranvier, where it plays a major role in AP generation and propagation, respectively. The high density of  $Na_v$  channels in the AIS versus soma has been under debate for several decades, mainly due to disagreements between results obtained using different experimental approaches. However, the more recent publications conclude that there are 30–50 times more  $Na_v1.6$  channels at the AIS than in the somatic compartment [43,56,57], which contributes to the lower threshold required for AP generation in this compartment [58]. The AIS is 10–60  $\mu\text{m}$  in length and characterized by a concentration of  $Na_v$  and  $K_v$  channels, cell adhesion molecules (L1 CAM, NrCAM, NF186, etc), cytosolic scaffolding proteins (AnkyrinG), a highly organized cytoskeleton (actin rings and microtubule fascicles), and microtubule-associated proteins such as TRIM46 (see reviews [59,60] for more details). Briefly, AnkyrinG (AnkG), a submembranous scaffolding protein with 270 and 480 KDa isoforms, is the major structural orchestrator of the AIS [61,62]. On its C-terminal side, it binds to microtubules through association with microtubule-associated proteins such as EB1/3 and Ndel1 [63,64]. On its N-terminal side, AnkG binds to  $\alpha\text{II}$ - and  $\beta\text{IV}$ - spectrins [62,65], which in turn associate with actin [66]. STORM super-resolution experiments demonstrated that actin, spectrin and AnkG form a periodic structure with actin filaments organized in rings spaced exactly 190 nm apart, which corresponds to the length of spectrin tetramers, and AnkG is located at the center of the spectrin tetramer [67,68]. AnkG also anchors  $Na_v$  and  $K_v7$  channels and cell adhesion molecules, which again present

a 190 nm striped pattern [67–69]. While Na<sub>v</sub> channels associate with AnkG through a 9 aa motif located in the intracellular II-III loop of Na<sub>v</sub> channels (Ankyrin Binding Motif (ABM)) [70,71], K<sub>v</sub>7.2 and K<sub>v</sub>7.3 bind to AnkG through a Na<sub>v</sub>-homologous motif located in their C-terminal domain [72]. Interestingly, K<sub>v</sub>1 channels are also concentrated at the AIS [73] and present a 190 nm striped pattern [74], but do not bind to AnkG, and instead they cluster at the AIS by interacting with the postsynaptic density-93 (PSD-93) scaffolding protein [75]. In some cells, K<sub>v</sub>2 channels and Ca<sub>v</sub> channels are also enriched at the AIS [76,77].

Na<sub>v</sub> channel concentration at the AIS via interaction with AnkG was demonstrated independently by two labs at almost the same time [70,71]. A motif located in the intracellular II-III loop of Na<sub>v</sub> channels was found to be sufficient for concentrating chimeric proteins (CD4, NF186 and K<sub>v</sub>2.1) to the AIS via AnkG binding. Garrido et al. demonstrated that 27 aa located at the Na<sub>v</sub>1.2 II-III loop (amino acids 1102–1028) governed compartmentalization of the CD4-Na<sub>v</sub>1.2 chimera at the AIS. Furthermore, over-expression of the soluble Na<sub>v</sub>1.2 II-III loop tagged with GFP decreased by half the sodium currents recorded in neurons, and dramatically decreased Na<sub>v</sub> localization at the AIS. Lemaillet et al. refined the ABM present in the II-III loop of Na<sub>v</sub> channels to just 9 aa (aa 1105–1113 for rNa<sub>v</sub>1.2) using both Na<sub>v</sub>1.2-GST pull-down experiments and chimera expression in hippocampal neuron cultures. Importantly, this 9 aa motif is conserved across all vertebrate Na<sub>v</sub> channels ((V/A)P(I/L)AXXE(S/D)D). Both studies indicated that the ABM was sufficient for localizing proteins to the AIS. However, almost 10 years passed before Gasser et al. demonstrated that the ABM was in fact necessary and sufficient for Na<sub>v</sub>1.6 localization at the AIS in vivo and in vitro [78]. Mutation of a single Na<sub>v</sub>1.6 amino acid (E1100A) centered within the ABM disrupted the localization of the channel not only to AIS but also to Nodes of Ranvier (in DRG neurons) [78]. Interestingly, no significant changes in electrophysiological properties were detected with this point mutant even though AnkG binding increases persistent current [79] and the equivalent residue in Na<sub>v</sub>1.5, when mutated, induces Brugada syndrome [80]. In summary, several studies support the

pivotal role of AnkG binding in the targeting of Na<sub>v</sub> channels to the AIS and the maintenance of neuronal polarity. Interestingly, CK2, a kinase able to form complexes with Na<sub>v</sub> channels, regulates AnkG-Na<sub>v</sub> interaction via phosphorylation within the ABM. Inhibition of CK2, reduces the localization of both Na<sub>v</sub>1 and AnkG to the AIS [81,82].

In addition to highly concentrating at the AIS, Na<sub>v</sub>1.6 also concentrates within nanodomains in the somato-dendritic compartment (Figure 2). Specifically, Na<sub>v</sub>1.6 forms nanoclusters of ≈230 nm on the soma of cultured rat hippocampal neurons expressing epitope-tagged Na<sub>v</sub>1.6. These structures are stable in place for over an hour but slowly gain and lose individual channels over this time frame [44]. While clustering is a prerequisite for coupled-gating, which has been suggested for some Na<sub>v</sub> channels [83], the functional significance of these somatic nanoclusters is unknown at this time. However, this localization is known to be AnkG independent since a Na<sub>v</sub>1.6 ABM mutant that does not localize to the AIS still forms somatic nanoclusters [44]. This result indicates multiple mechanisms underlie Na<sub>v</sub> channel localization in neurons and adds to the mystery of neuronal complexity. How do neurons maintain such different localizations of Na<sub>v</sub>1.6? Is it a matter of different interaction partners? Is the decision made at early stages of biosynthesis, at the vesicular transport level, or at the plasma membrane? How functionally different are somatic Na<sub>v</sub>1.6 channels as compared to those in the AIS or Nodes of Ranvier?

### ***Na<sub>v</sub> trafficking mechanisms***

Na<sub>v</sub> channels, as most other transmembrane plasma membrane proteins, are translated in the rough endoplasmic reticulum (ER). If quality control misfolding checkpoints are passed, and after glycosylation (which takes place in both the ER and Golgi apparatus), they are trafficked to the neuronal surface via vesicular transport [84,85]. In fact, there are several disease-related mutations in Na<sub>v</sub>1.6 that are good examples of the importance of such early biosynthesis steps (see section below for more details).

Specific mechanisms must exist in order to guarantee the delivery of a specific ion channel to a determined compartment such as the soma or

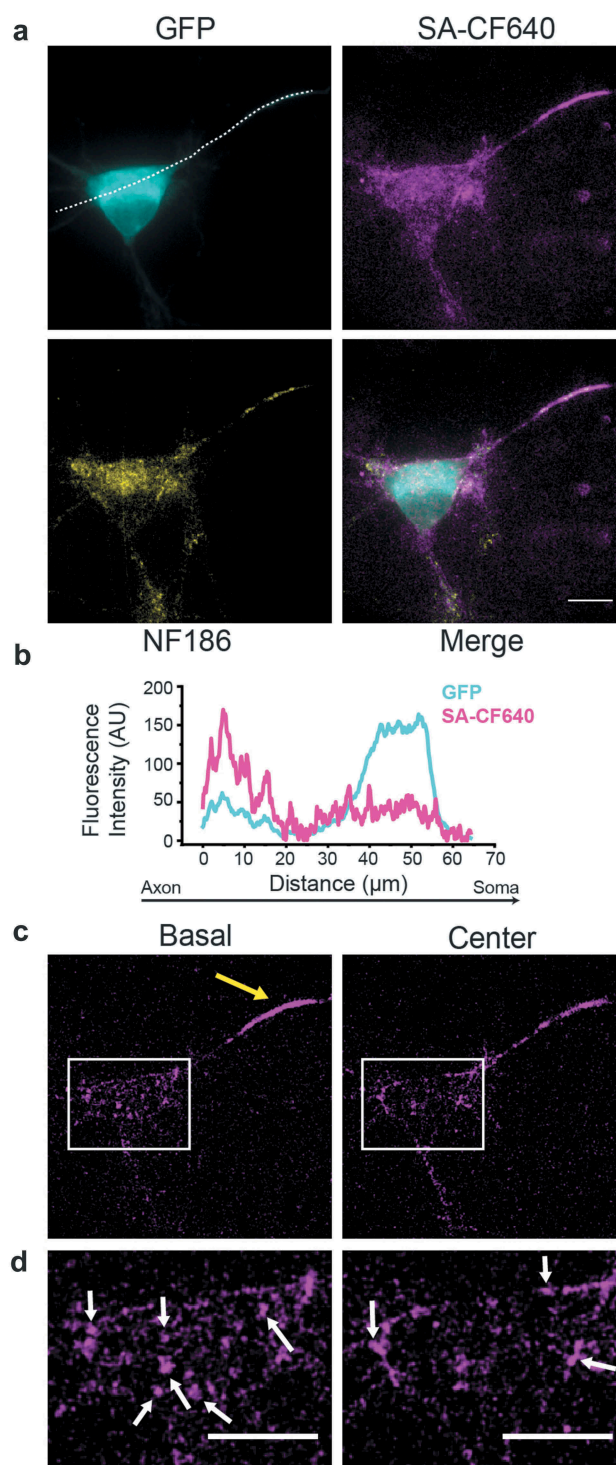


**Figure 2.  $\text{Na}_v1.6$  is concentrated at the AIS of rat hippocampal neurons (rHN), while presenting a punctate pattern (nanoclusters) on the soma.** Transfected DIV7 rHN expressing  $\text{Na}_v1.6$  tagged with an extracellular biotinylation site and cytoplasmic GFP. **A)** Average projections of a z-stack acquired with a spinning disk confocal of GFP (cyan), surface labeled  $\text{Na}_v1.6$  channels (magenta), and NF186 (yellow). White dashed line defines the profile presented in B. **B)** Line profile of the fluorescence intensities of GFP and surface labeled channels across the axon and somatic compartment. **C)** Individual images corresponding to basal (left) and center (right) planes of the same neuron shown in panel A. Large yellow arrow indicates the AIS. **D)** Enlargement of the somatic compartments (white squares shown in panel C). White arrows indicate somatic  $\text{Na}_v1.6$  nanoclusters. All scale bars represent 10  $\mu\text{m}$ .

the AIS. The transport of  $\text{Na}_v$  channels to the cell surface and how neurons accomplish and maintain such a polarized distribution has been under debate since the early 2000s. As summarized in Figure 3, at least three different mechanisms could target  $\text{Na}_v$  channels to the soma and AIS: 1) preferential somatic delivery followed by lateral diffusion into the AIS and immediate immobilization upon AnkG binding; 2) random delivery of protein into both compartments, followed by specific somatic endocytosis; and 3) directed delivery into each compartment with a preference for the AIS due to the requirement here for a high channel concentration. However, given the complexity of biology, it is likely some combination of all three mechanisms exists.

The AIS being a diffusion trap (trapping channels that were delivered initially in the somatic compartment [86]) (mechanism 1) avoids the need for any vesicular delivery into the axon in order to get  $\text{Na}_v$  channels into the AIS. However, this idea requires free diffusion between the soma and AIS. Experiments performed in the early 90s indicated that a plasma membrane diffusion

barrier exists between the somatic and axonal compartments [87,88]. The physiological role of this barrier was naturally assumed to be central to neuronal polarization. This barrier blocked the trans-compartment diffusion of not only membrane proteins but also membrane lipids, and was fully established in cultured neurons by DIV10, as demonstrated by single particle tracking experiments performed in the early 2000s with labeled phospholipids and ion channel chimeras [89,90]. It is difficult to imagine how a large membrane protein such as a  $\text{Na}_v$  channel could make it across this barrier in a mature neuron. However, since  $\text{Na}_v$  channel expression begins well before DIV7 [89] this mechanism could play a role in the early development of the AIS.

The random delivery and soma specific endocytosis mechanism (mechanism 2) was supported by experiments performed with CD4- $\text{Na}_v$ 1.2 chimeras in both COS7 cells and hippocampal neurons [91]. Garrido et al. showed that the C-terminal motif of  $\text{Na}_v$ 1.2 governed the axonal compartmentalization of a CD4- $\text{Na}_v$ 1.2C-terminus chimera, which was inserted into both the somato-dendritic and the

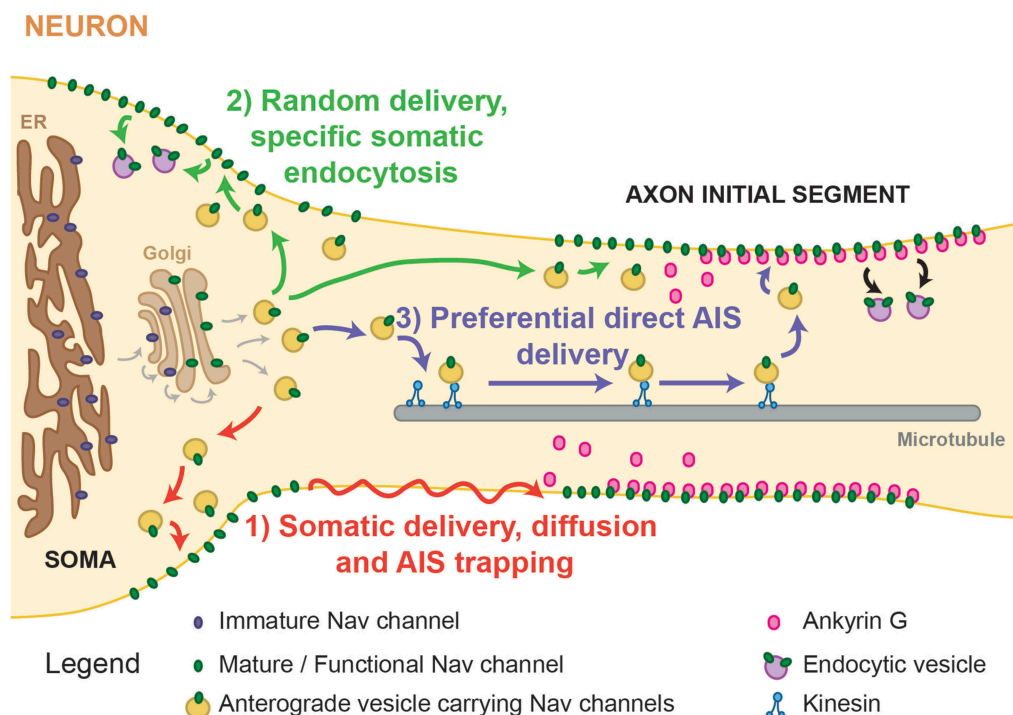


**Figure 3. AIS localization and  $\text{Na}_v$  trafficking mechanisms.** Possible trafficking mechanisms involved in  $\text{Na}_v$  localization in the somatic (left) and AIS (right) compartments: 1) preferential somatic delivery followed by lateral diffusion into the AIS and immediate immobilization upon AnkG binding (red arrows); 2) random delivery of protein into both compartments, followed by specific somatic endocytosis (green arrows); 3) directed delivery into each compartment with a preference for the AIS (blue arrows).

axonal compartments and was later removed from the soma but retained in the AIS. Within the Na<sub>v</sub>1.2 C-terminus resides a di-leucine motif (IL1857–1858), which was proposed to be involved in clathrin-dependent endocytosis of the chimera from the somatic compartment and dendrites. The idea at the time was that either axonal Na<sub>v</sub>1.2 channels were prevented from endocytosis due to binding an axonal partner (such as AnkG) or that the axonal and somato-dendritic endosomal pathways were differentially regulated. Interestingly, although Na<sub>v</sub>1.1 and Na<sub>v</sub>1.6 also contain such di-leucine motif, it did not seem to play a role in these channels' localization. The authors speculated that this could be due to either this motif not being exposed in the case of Na<sub>v</sub>1.1 or Na<sub>v</sub>1.6 (due to divergence in the C-terminal domain sequence and different conformations that may be adopted) or the different isoforms interacted with different endogenous partners. Also, related to Na<sub>v</sub> channel endocytosis, Na<sub>v</sub> channels contain a PY motif within their C-terminal domain which can be ubiquitinated by Nedd4 and Nedd4-2, and which induce protein degradation [92]. Fotia et al. demonstrated that Na<sub>v</sub>1.2 and Na<sub>v</sub>1.7 were ubiquitinated and, in *Xenopus* oocytes, while Nedd4-2 decreased the activity of Na<sub>v</sub>1.2, Na<sub>v</sub>1.7 and Na<sub>v</sub>1.8, Nedd4 only inhibited Na<sub>v</sub>1.2 and Na<sub>v</sub>1.7, not Na<sub>v</sub>1.8. Such endocytosis mechanisms were suggested to be involved in the Na<sub>v</sub> channel polarized distribution in neurons. Some years later, Fache et al., continued supporting the idea of random insertion and somatic endocytosis with the publication that another motif (17 aa upstream of the ABM) was required for endocytosis of CD4-Na<sub>v</sub> chimeras (in COS7 and neuronal cells) [93], and that probably the high concentration of AnkG in the AIS tethered the CD4-Na<sub>v</sub>1.2 II-III linker chimera and protected it from endocytosis. However, a concern with these results centered on whether the mechanism described for the CD4 chimeras would be translatable to the full-length Na<sub>v</sub>1.2. Indeed, this is why Gasser et al. performed the experiments with full Na<sub>v</sub>1.6 channel previously described. Although these investigators did not directly address delivery or endocytosis, they did demonstrate that AnkG binding was necessary and sufficient for native Na<sub>v</sub>1.6 localization at the AIS [78]. Importantly,

they also paved the way for trafficking experiments with complete Na<sub>v</sub> channels.

In order to address Na<sub>v</sub> channel delivery directly into the AIS membrane (mechanism 3), our lab developed fluorescent protein tagged Na<sub>v</sub>1.6 channels that also carried a biotinylation site on the extracellular surface [56]. Biotinylation of this extracellular lysine occurred in the ER lumen during biosynthesis, thus these channels were biotinylated before they reached the plasma membrane. This extracellular biotin allowed for the specific detection of surface channels in living neurons using fluorescently conjugated streptavidins (see Figure 2 for an example). Importantly, if cultured neurons were incubated with fluorescent streptavidin during high signal to noise TIRF imaging, the delivery location of nascent channels to the cell surface would be detected with single molecule sensitivity [56]. Using this approach, we demonstrated that the full length Na<sub>v</sub>1.6 was preferentially inserted into the AIS membrane via direct vesicular trafficking (up to 6 channels/vesicle). Once inserted at the AIS plasma membrane, channels were immediately immobilized, as demonstrated by both FRAP and single particle tracking experiments. Such immediate immobilization did not occur to channels that were delivered at the somatic compartment. Furthermore, single particle tracking experiments also proved that no channels crossed the somato-axonal barrier, further arguing against the diffusion trap mechanism discussed above. An ABM Na<sub>v</sub>1.6 mutant was not preferentially delivered to the AIS, and the channels that were delivered to AIS were not immobilized. It was surprising that this mutant was delivered to the AIS at all since the Gu lab had demonstrated that AnkG links Na<sub>v</sub>1.2 to KIF5 to facilitate vesicular transport into the axon [94]. Thus, it appears different Na<sub>v</sub> isoforms are trafficked via distinct mechanisms. Interestingly, although the ABM motif was required for preferential delivery to the AIS it did not confer preferential AIS delivery when added to a Na<sub>v</sub>1.2-K<sub>v</sub>2.1 chimera, indicating other channel domains are likely involved [56]. In addition, the use of the surface-specific label for Na<sub>v</sub>1.6 (biotinylated loopBAD tag, labeled with CF640-conjugated streptavidin), combined with the sensitivity of TIRF imaging, indicated that besides its

concentration at the AIS,  $\text{Na}_v1.6$  presents two populations in the somatic compartment, a static nano-clustered pattern against a background of freely diffusing  $\text{Na}_v1.6$  molecules (see Figure 2). Nano-cluster formation was still observed with the ABM mutant incapable of binding AnkG [44,56]. In summary, our newly developed  $\text{Na}_v1.6$  constructs, which permitted the live imaging of single channels on the neuronal surface, allowed for both the mapping of membrane insertion at the AIS and the discovery of ankyrin-independent  $\text{Na}_v1.6$  localization on the somatic surface.

The AIS delivery experiments just described suggested that endocytosis plays little role in the compartmentalization of  $\text{Na}_v1.6$  localization. However, biology is not always simple, as was reinforced when we applied our imaging technology to  $\text{Na}_v1.6$  mutants previously reported to have forward trafficking defects. One such  $\text{Na}_v1.6$  mutant (MAPM) carried amino acid substitutions in its MAP1B binding domain [28]. MAP1B light chain interaction with wild-type  $\text{Na}_v1.6$  was demonstrated by both yeast two-hybrid experiments and co-immunoprecipitation from mouse brain membranes. The MAP1B binding motif was defined in the N-terminal domain of  $\text{Na}_v1.6$  (VAVP, amino acids 77–80) [95]. It was initially postulated that MAP1B binding was necessary for

delivery of  $\text{Na}_v1.6$  to the surface since removal of MAP1B binding prevented the detection of  $\text{Na}_v1.6$  currents in transfected ND7/23 cells. It was reasonable to assume that MAP1B binding was involved in the forward trafficking of  $\text{Na}_v1.6$  since, in addition to its classical role in microtubule stabilization, MAP1B is also known to regulate the localization, function and trafficking of different channels and receptors [96]. However, as our recent work demonstrated, and to our surprise, the  $\text{Na}_v1.6$  MAPM traffics to the somatic surface of hippocampal neurons but is not concentrated within the AIS (Figure 4(a)) [28]. While we expected that this distribution was due to a lack of trafficking to the AIS, the fluorescent biotinylation assay described above confirmed that this was not the case, with the MAPM being readily delivered to the AIS surface where it was immediately immobilized just like the wild-type channel. We found that MAPM is not concentrated at the AIS because, without MAP1B binding, it is internalized via compartment-specific  $\text{Na}_v1.6$  endocytosis [28]. Although MAPM channels are still tethered at the AIS plasma membrane by AnkG binding (as demonstrated by their restricted diffusion, similar to wild-type  $\text{Na}_v1.6$  channels), these channels are endocytosed from the axonal compartment when MAP1B is not able to bind to  $\text{Na}_v1.6$  (as illustrated

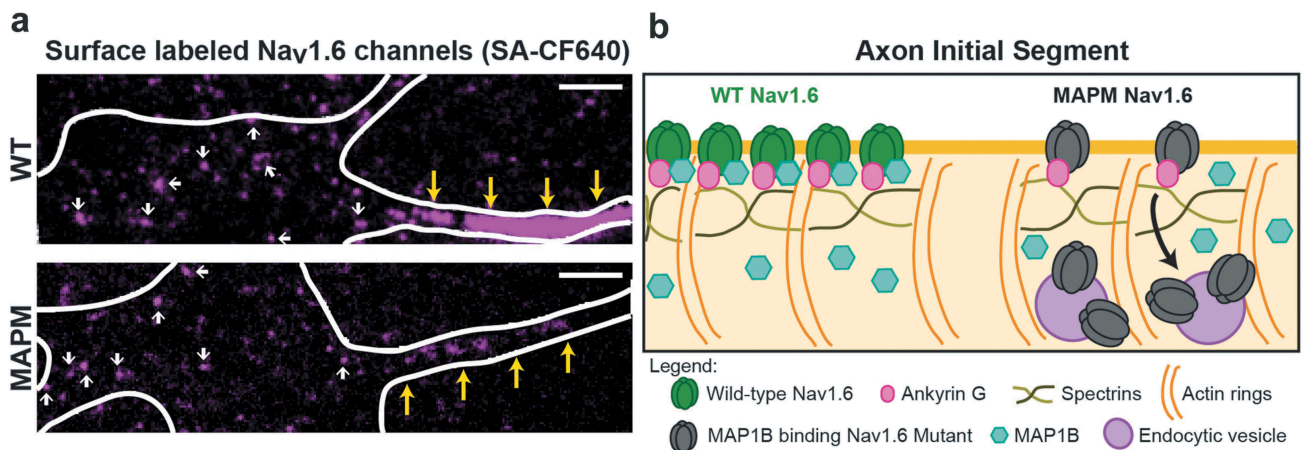


**Figure 4. MAP1B binding prevents  $\text{Na}_v1.6$  AIS compartment-specific endocytosis. A)** TIRF images of DIV10 rHNs transfected with WT (top) or MAPM (bottom)  $\text{Na}_v1.6$ LoopBADGFP (only surface labeled channels with CF640-conjugated streptavidin (SA-CF640) are shown). White line depicts the cell outline. Yellow arrows point to the AIS (identified by NF186 labeling (data not shown)). Smaller white arrows point to somatic nano-clusters. Notice that while no significant differences are noticeable in the somatic labeling, there is a drastic decrease in the AIS labeling with MAPM versus WT channels. Scale bars represent 5  $\mu\text{m}$ . **B)** Schematic drawing showing that while AIS WT  $\text{Na}_v1.6$  channels (green), are not endocytosed, AIS MAPM channels (p.VAVP(77–80)AAAA) (black) are, although they can still bind to AnkG.

in Figure 4(b)). Clearly, there is still much we do not understand about the regulation of the  $\text{Na}_v$ -AnkG interaction. This trafficking work had an unexpected functional bonus as it also suggested that there is a correlation between  $\text{Na}_v1.6$  channel function and its location, where  $\text{Na}_v1.6$  persistent current is regulated by subcellular location. Both the MAPM and ABM mutants (both mainly somatic channels) presented five times more persistent current than wild-type  $\text{Na}_v1.6$ , which accumulates at the AIS [28].

During the last two decades, the observation that somato-dendritic cargo-carrying vesicles do not enter the AIS has emphasized the importance/existence of a cytoplasmic filter regulating cargo entry into the axon [97–99]. This filter, which is formed during axon maturation (DIV3–5) [98], seems to be another complex mechanism formed by the coordination of different elements, one of them being the actin cytoskeleton, where dendritic protein-carrying vesicles are stopped [100,101]. This proximal pre-axonal exclusion zone (PAEZ) is also rich in MAP2 and TRIM46, is AnkG independent but dependent on microtubules and microtubule motors. Here, the combination of motor proteins associated with a particular vesicle determines what can enter the axon [102–105]. In addition, the recruitment of myosin-V to certain vesicles can induce vesicle immobilization at the PAEZ [106]. Hopefully, within the next years the detailed mechanisms underlying this selective cargo transport into the axon will be elucidated.

Another aspect of  $\text{Na}_v$  cell biology that needs more development centers on the molecular motors involved in vesicle transport. Although the role of kinesins in ion channel and AMPA receptor transport had been known since the mid 2000s [107,108], it wasn't until 2013 that an interaction between KIF5 and a  $\text{Na}_v$  channel and forward trafficking was demonstrated [109]. Su et al. demonstrated that  $\text{Na}_v1.8$  interacts (directly or indirectly) with amino acids 511–620 in KIF5B, promoting surface channel expression via forward trafficking and also preventing channel degradation, without altering the biophysical properties of the channel [109]. Although KIF5A was also able to bind to  $\text{Na}_v1.8$ , KIF5B showed a stronger affinity. Interestingly, KIF5 interacted with both  $\text{Na}_v1.8$  and  $\text{Na}_v1.9$  in dorsal root ganglia (DRG) neurons, but not with  $\text{Na}_v1.6$  or  $\text{Na}_v$

1.7 [109]. A few years later, direct interaction between KIF5B and AnkG (but not AnkB) was reported, and AnkG was found to be required for  $\text{Na}_v1.2$  to be transported to the AIS.  $\text{Na}_v1.2$  co-transport with KIF5 was observed, as well as co-transport with AnkG in a subset of rat hippocampal neurons [94]. KIF5 and  $\text{Na}_v1.2$  bind distinct AnkG domains, which allows AnkG to act as an adaptor protein between the motor and channel. Unfortunately, in this study, no other  $\text{Na}_v$  channel isoforms were tested, so it is unknown whether  $\text{Na}_v1.6$  also needs to be bound to AnkG to be transported into the axon by KIF5, or whether it is transported by another kinesin. However, according to our experiments, an ABM  $\text{Na}_v1.6$  mutant was still delivered (although not preferentially) to the AIS [56], suggesting that this isoform does not require AnkG as an adaptor. Interestingly, a recent report indicates that  $\text{Na}_v1.6$  is transported to the surface of sensory neurons by a tripartite complex  $\text{Na}_v1.6/\delta$ -catenin/KIF3A (as observed by SIM super-resolution three color colocalization experiments) [110], although the authors did not determine whether such interactions were direct or indirect through other proteins. Palmitoylation of  $\delta$ -catenin facilitated the membrane-directed trafficking of  $\text{Na}_v1.6$  in DRG neurons. They also showed by immunoprecipitation experiments that  $\delta$ -catenin was able to bind to  $\text{Na}_v1.6$  and  $\text{Na}_v1.7$  (but not  $\text{Na}_v1.8$  nor  $\text{Na}_v1.9$ ) and KIF3A or KIF3B (but rarely KIF5A, KIF5B, KIF17 and KIFC2). Myosin-II (myh9 and myh10) has also been described to interact with  $\text{Na}_v1.2$ ,  $\text{Na}_v1.3$ ,  $\text{Na}_v1.7$  and  $\text{Na}_v1.8$ , but not with  $\text{Na}_v1.1$ ,  $\text{Na}_v1.6$  nor  $\text{Na}_v1.9$  (according to immunoprecipitation experiments from rodent brain tissues) [111]. After analyzing the electrophysiological properties of  $\text{Na}_v1.8$  with and without myh10 in ND7/23 cells, where a 3-fold increase in current density and changes in activation and inactivation curves were observed, the authors suggested that non-muscle myosin-II could interact with  $\text{Na}_v$  channels to facilitate/regulate their transport and function.

### **AIS plasticity**

Besides its complex and organized structure, AIS location and composition is much less static than was initially appreciated. The AIS is dynamically regulated on both short and long term timescales,

either by biophysical changes in ion channel function (which occur in the scale of milliseconds to seconds) or structural reorganization of the AIS (also called AIS plasticity, and which occurs in the scale of hours to days). These changes are expected to contribute to fine adjustments of cellular and network activity. Any mechanism involved in ion channel trafficking and AIS assembly is also likely to be involved in AIS plasticity.

The first report of AIS plasticity was by Grubb and Burrone in 2010. They reported that after depolarization (either treatment of hippocampal neurons with 15 mM KCl for 48 h, or photo stimulation-induced activation of channelrhodopsin2), the AIS moved up to 17  $\mu\text{m}$ . This distal shift was also observed for AnkG,  $\beta\text{IV}$ -spectrin, NF186, FGF14 and, most importantly,  $\text{Na}_v$  channels. AIS plasticity was  $\text{Na}_v$  activity independent (TTX did not prevent the shift) but dependent on  $\text{Ca}_v$  channels. AIS translocation was accompanied by decreased neuronal excitability and a correlation existed between the AIS start position and number of spikes generated, showing that neurons with a more proximal AIS presented a lower threshold for AP initiation and also more spikes in response to input current [112]. This publication was followed by another report showing that in avian brainstem auditory neurons, days after deprivation of auditory inputs, the AIS became longer, without affecting its proximal location and  $\text{Na}_v$  channel density [113]. This size increase led to increased neuronal excitability. Interestingly, the extent of AIS elongation correlated with the levels of auditory/sensory attenuation that were induced. Such elongation was accompanied by changes in expression of  $\text{K}_v$  channels:  $\text{K}_v7.2$  increased while  $\text{K}_v1.1$  decreased, with no changes in  $\text{K}_v3.1$  [114]. Some years later, a detailed pharmacological screening performed by the Grubb laboratory concluded that AIS relocation in rat hippocampal cultures was triggered by activation of only L-type  $\text{Ca}_v1$  channels and CaMKII and was also calcineurin dependent (but calcpain, PKA, PKC, MAPKK, p38 and PI3K independent) [115]. Interestingly, although calcineurin was necessary and sufficient for AIS relocation, the authors did not find a calcineurin concentration at the AIS.

Recently, the non-muscle myosin-II has been suggested to be necessary for AIS plasticity

[116,117]. Treatment with blebbistatin (a myosin-II ATPase inhibitor) blocked both the activity-dependent translocation and shortening of the AIS induced by 15 mM KCl [116]. Interestingly, while myosin-II is present at the AIS, it is not concentrated there. However, the phosphorylated form of the myosin-II light chain (pMLC) is concentrated at the AIS, and in fact, pMLC is associated with the actin rings in the AIS [116,117]. Furthermore, as a result of a sustained depolarization, pMLC levels were specifically and rapidly decreased at the AIS, which preceded actin disorganization and loss of immuno-staining of AnkG and  $\text{Na}_v$  channels. The authors demonstrated that actin stabilization with either phalloidin or jasplakinolide prevented the activity-dependent loss of AnkG, but not the loss pMLC, suggesting that the loss of pMLC is regulated by a distinct mechanism [117].

Besides the slowly responding AIS plasticity just discussed (taking place within 3–6 hours and even days), fast AIS plasticity has also been reported. For example, high glutamate concentrations induced dynamin and clathrin-coated pit dependent endocytosis of  $\text{K}_v7.2$  and  $\text{K}_v7.3$  and  $\text{Na}_v$  channels in hippocampal neurons within 10 minutes. These processes required the activation of NMDA receptors, resulting in calcium influx and calcpain activation; while being calcineurin, PP1, PP2A and CaMKII kinase independent [118]. Such endocytosis seemed to be selective to AnkG-binding proteins, since AIS-localized GABA receptors were not endocytosed (although declustering was observed). It is important to note that the authors did not use a complete  $\text{Na}_v$  channel for this experiment, instead they used a SEP-TAC- $\text{Na}_v1.2$  II-III loop chimera reporter (which bound to AnkG). Thus it is not clear whether their results would apply to full  $\text{Na}_v1.2$  and  $\text{Na}_v1.6$ .

Forms of AIS plasticity have also been observed under pathological conditions. For example, AIS integrity is disrupted in ischemia (in a calcpain-dependent manner) and during chronic microglial inflammation (a ROS-producing enzyme, NOX2-mediated and calcpain-dependent process) [119–121]. Remodeling and shortening of the AIS length has been observed after stroke [122]. A shortening of the AIS in medial prefrontal cortex and hippocampus has also been observed in *db/db* mice (an

established animal model for type-2 diabetes), which could lead to a decreased neuronal excitability that could explain cognitive and mood impairments associated with type-2 diabetes [123]. AIS plasticity has also been observed in cases of demyelination, epilepsy and Angelman syndrome (a neurodevelopmental disorder associated with autism) (for a review see [124]). AIS plasticity seems to be bidirectional and a homeostatic process that allows neurons to control their excitability and neuronal output [125]. It has also been theorized that since neuronal excitation increases during aging, aged neurons may present a shorter and/or more distal AIS. Although controversial, there are a couple of reports that support this theory [126,127].

AIS plasticity appears to be somehow cell-type-specific. For instance, all excitatory hippocampal neurons seem to present AIS plasticity, while GABAergic inhibitory hippocampal neurons do not [115]. When dopaminergic neurons from olfactory bulb (OB) were depolarized for 24h, their AIS lengthened and relocated proximally toward the soma, contrary to what was observed in other non-GABAergic OB neurons and hippocampal cells (shorter length and distal shift). Such translocation was dependent on L-type  $Ca_v$  channels but calcineurin, CaMKII and PKA independent. OB dopaminergic neurons treated with TTX for 24h did not present a shift but the AIS became shorter [128]. AIS plasticity has also been observed in human neurons. While chronic depolarization shortened the AIS of human cortical excitatory neurons [129], a distal shift of the AIS was observed in hiPSC-derived neurons (heterogeneous culture of excitatory and inhibitory neurons) [130]. Curiously, the shortening of human AIS was related to EB3 levels.

Furthermore, there is differential ion channel expression between distinct cell types, which also changes during development along with AIS location and structural components [131]. For example, while  $Na_v1.2$  is expressed early in the AIS during development, it is later displaced by  $Na_v1.6$ , as the AIS becomes shorter and more distal. Furthermore,  $Na_v1.2$ , like  $Na_v1.1$ , presents a more proximal location than  $Na_v1.6$  even though AnkG is evenly distributed along the AIS [132,133]. Taken together these facts, and our recent discovery that MAP1B binding to N-terminal of  $Na_v1.6$

prevents its endocytosis from the AIS [28], raises the possibility that MAP1B could play a role in this differential isoform location or even AIS plasticity.  $Na_v1.6$  is the only isoform with a VAVP sequence in its MAP1B binding motif and yeast two-hybrid experiments showed that the  $Na_v1.1$  N-terminal domain (with a VSEP) does not bind MAP1B [95]. It will be interesting to see if the MAP1B endocytosis-shielding effect is extended to other isoforms and whether it plays a role in AIS plasticity (although bulk endocytosis does not seem to play a role in AIS shortening [116]).

### **Impaired $Na_v$ trafficking/AIS related disease-causing mutations**

Most channelopathies (diseases caused by ion channel defects) are due to mutations affecting channel function, trafficking, or both. Most  $Na_v$  mutation-causing diseases are associated with a change in the conducting properties of the channel rather than altered trafficking (for reviews see [134–138]), but in this section we will focus on the latter. As mentioned earlier, disruption of AIS  $Na_v$  localization has been observed in cases of ischemia, demyelination, epilepsy and Angelman Syndrome [124,139].

Since early  $Na_v$  biosynthesis steps (exiting the ER and Golgi in order to reach to the plasma membrane) are crucial, it is not surprising that several disease-related mutations in  $Na_v1.6$  are caused by trafficking pathway defects. For example, the mouse *ataxia3*-causing mutation S21P in  $Na_v1.6$  does not generate sodium currents when expressed in ND7/23 cells unless cells are incubated at 30°C instead of 37°C, indicating a temperature-dependent trafficking defect. Immuno-staining of primary cerebellar granule cells from the *ataxia3* mice showed that the mutant was retained at the cis-Golgi level [140]. The human epilepsy-causing mutation R223G in  $Na_v1.6$  also leads to almost no channel expression and it is also partially rescued by incubating cells at 30°C instead of 37°C [141]. On the other hand, the spontaneous mouse mutation I1750Δ generates reduced sodium channel activity, due to defective glycosylation of the channel that results in improper localization at AIS and Nodes of Ranvier, leading to mice with movement disorders [142].

Na<sub>v</sub>1.6 is not the only Na<sub>v</sub> channel where mutations that impair trafficking cause disease. For example, R1648C and G1674R Na<sub>v</sub>1.1 mutants (associated with Dravet Syndrome [143]) presented less surface channel and reduced current density when expressed in HEK293 cells. Interestingly, incubation with antiepileptic drugs for 24h increased surface expression in a mutant specific manner. For example, phenytoin and lamotrigine promoted trafficking of R1648C, while only phenytoin affected the G1674R mutant [143]. Furthermore, M1841T Na<sub>v</sub>1.1, a mutation associated with familial epilepsy, is a loss-of-function mutation that impairs forward trafficking to the surface, but surface expression can be restored by incubation at <30°C [144]. Mutation D1639N in Na<sub>v</sub>1.8, identified in a human patient suffering from a chronic pain syndrome (Small Fiber Neuropathy) [145], impairs trafficking of Na<sub>v</sub>1.8 to the plasma membrane [146]. Interestingly, the authors were able to restore its trafficking, *in vitro*, by overnight treatment with lidocaine. Mutations in Na<sub>v</sub>1.5 that affect either glycosylation or protein folding of the cardiac channel are associated with Brugada syndrome and Long QT syndrome [147–149]. In some cases, trafficking was improved by treatment with mexiletine.

Trafficking based diseases can be caused by mutations in proteins other than Na<sub>v</sub> channels themselves. For example, AnkG polymorphisms are associated with a higher risk of bipolar disorder [150,151] and intellectual disabilities [152]. Recently, three human mutations in ANK3 (the gene encoding for the 480 KDa isoform of AnkG), caused improper AIS development manifested by a reduced Na<sub>v</sub> channel and NF186 concentration within AIS [153]. These mutations are associated with neurodevelopmental disorder with delayed speech, intellectual impairment, and seizures, among other phenotypes.

### Future directions

Although remarkable progress has been made during the last decade regarding Na<sub>v</sub> trafficking and AIS structure, there are still numerous questions that remain to be answered. What is the functional role of the somatic Na<sub>v</sub>1.6

nanoclusters and how are they maintained in the absence of AnkG binding? What determines whether a Na<sub>v</sub>1.6 channel reaches the plasma membrane at the somatic or axonal compartment? Are these mechanisms specific for each Na<sub>v</sub> isoform or do all isoforms use the same motors and/or adaptor proteins? What is the specific molecular machinery involved in AIS plasticity? For example, does axonal endocytosis and the regulation of MAP1B binding play a role in AIS plasticity? Hopefully within the next years some of these questions will be answered. A better understanding of the complexity of Na<sub>v</sub> localization and AIS plasticity will shed light on how this neuronal compartment regulates neuronal activity in health and disease.

### Acknowledgments

The authors thank Ashley Leek and Emily Maverick for critical review of the manuscript. This work was supported by NIH grant RO1 NS085142 awarded to MMT; and by NIH/NCATS Colorado CTSA Grant Number UL1 TR002535 awarded to LS.

### Disclosure statement

No potential conflict of interest was reported by the authors.

### Funding

This work was supported by the National Institutes of Health under Grant RO1 NS085142; and NIH/NCATS Colorado CTSA under Grant UL1 TR002535. Contents are the authors' sole responsibility and do not necessarily represent official NIH views.

### References

- [1] Catterall WA. Voltage-gated sodium channels at 60: structure, function and pathophysiology. *J Physiol.* 2012;590(11):2577–2589.
- [2] de Lera Ruiz M, Kraus RL. Voltage-gated sodium channels: Structure, function, pharmacology, and clinical indications. *J Med Chem.* 2015;58(18):7093–7118.
- [3] O'Malley HA, Isom LL. Sodium channel beta subunits: emerging targets in channelopathies. *Annu Rev Physiol.* 2015;77:481–504.
- [4] Agnew WS, Moore AC, Levinson SR, et al. Identification of a large molecular weight peptide associated with a tetrodotoxin binding protein from the electroplax of *Electrophorus electricus*. *Biochem Biophys Res Commun.* 1980;92(3):860–866.

- [5] Hodgkin AL, Huxley AF. A quantitative description of membrane current and its application to conduction and excitation in nerve. *J Physiol.* **1952**;117(4):500–544.
- [6] Hodgkin AL, Huxley AF. Currents carried by sodium and potassium ions through the membrane of the giant axon of *Loligo*. *J Physiol.* **1952**;116(4):449–472.
- [7] Hodgkin AL, Huxley AF. The components of membrane conductance in the giant axon of *Loligo*. *J Physiol.* **1952**;116(4):473–496.
- [8] Beneski DA, Catterall WA. Covalent labeling of protein components of the sodium channel with a photoactivable derivative of scorpion toxin. *Proc Natl Acad Sci USA.* **1980**;77(1):639–643.
- [9] Hartshorne RP, Catterall WA. Purification of the saxitoxin receptor of the sodium channel from rat brain. *Proc Natl Acad Sci USA.* **1981**;78(7):4620–4624.
- [10] Tamkun MM, Talvenheimo JA, Catterall WA. The sodium channel from rat brain. Reconstitution of neurotoxin-activated ion flux and scorpion toxin binding from purified components. *J Biol Chem.* **1984**;259(3):1676–1688.
- [11] Catterall WA. Localization of sodium channels in cultured neural cells. *J Neurosci.* **1981**;1(7):777–783.
- [12] Noda M, Shimizu S, Tanabe T, et al. Primary structure of electrophorus electricus sodium channel deduced from cDNA sequence. *Nature.* **1984**;312(5990):121–127.
- [13] Kayano T, Noda M, Flockerzi V, et al. Primary structure of rat brain sodium channel III deduced from the cDNA sequence. *FEBS Lett.* **1988**;228(1):187–194.
- [14] Noda M, Ikeda T, Kayano T, et al. Existence of distinct sodium channel messenger RNAs in rat brain. *Nature.* **1986**;320(6058):188–192.
- [15] Vassilev PM, Scheuer T, Catterall WA. Identification of an intracellular peptide segment involved in sodium channel inactivation. *Science.* **1988**;241(4873):1658–1661.
- [16] Stuhmer W, Conti F, Suzuki H, et al. Structural parts involved in activation and inactivation of the sodium channel. *Nature.* **1989**;339(6226):597–603.
- [17] Noda M, Suzuki H, Numa S, et al. A single point mutation confers tetrodotoxin and saxitoxin insensitivity on the sodium channel II. *FEBS Lett.* **1989**;259(1):213–216.
- [18] Kellenberger S, Scheuer T, Catterall WA. Movement of the Na<sup>+</sup> channel inactivation gate during inactivation. *J Biol Chem.* **1996**;271(48):30971–30979.
- [19] Heinemann SH, Terlau H, Stühmer W, et al. Calcium channel characteristics conferred on the sodium channel by single mutations. *Nature.* **1992**;356(6368):441–443.
- [20] Cestele S, Yarov-Yarovoy V, Qu Y, et al. Structure and function of the voltage sensor of sodium channels probed by a beta-scorpion toxin. *J Biol Chem.* **2006**;281(30):21332–21344.
- [21] Armstrong CM, Bezanilla F. Currents related to movement of the gating particles of the sodium channels. *Nature.* **1973**;242(5398):459–461.
- [22] Claes L, Del-Favero J, Ceulemans B, et al. De novo mutations in the sodium-channel gene *SCN1A* cause severe myoclonic epilepsy of infancy. *Am J Hum Genet.* **2001**;68(6):1327–1332.
- [23] Escayg A, MacDonald BT, Meisler MH, et al. Mutations of *SCN1A*, encoding a neuronal sodium channel, in two families with GEFS+2. *Nat Genet.* **2000**;24(4):343–345.
- [24] Wang Q, Shen J, Splawski I, et al. *SCN5A* mutations associated with an inherited cardiac arrhythmia, long QT syndrome. *Cell.* **1995**;80(5):805–811.
- [25] Zhang X, Ren W, DeCaen P, et al. Crystal structure of an orthologue of the NaChBac voltage-gated sodium channel. *Nature.* **2012**;486(7401):130–134.
- [26] Payandeh J, Scheuer T, Zheng N, et al. The crystal structure of a voltage-gated sodium channel. *Nature.* **2011**;475(7356):353–358.
- [27] Payandeh J, Gamal El-Din TM, Scheuer T, et al. Crystal structure of a voltage-gated sodium channel in two potentially inactivated states. *Nature.* **2012**;486(7401):135–139.
- [28] Sole L, Wagnon JL, Akin EJ, et al. The MAP1B binding domain of Nav1.6 is required for stable expression at the axon initial segment. *J Neurosci.* **2019**;39(22):4238–4251.
- [29] Akin EJ, Higerd GP, Mis MA, et al. Building sensory axons: delivery and distribution of Nav1.7 channels and effects of inflammatory mediators. *Sci Adv.* **2019**;5:eaax4755.
- [30] Schaller KL, Krzemien DM, Yarowsky PJ, et al. A novel, abundant sodium channel expressed in neurons and glia. *J Neurosci.* **1995**;15(5 Pt 1Pt 1):3231–3242.
- [31] Goldin AL, Snutch T, Lubbert H, et al. Messenger RNA coding for only the alpha subunit of the rat brain Na channel is sufficient for expression of functional channels in xenopus oocytes. *Proc Natl Acad Sci U S A.* **1986**;83(19):7503–7507.
- [32] Burgess DL, Kohrman DC, Galt J, et al. Mutation of a new sodium channel gene, *Scn8a*, in the mouse mutant ‘motor endplate disease’. *Nat Genet.* **1995**;10(4):461–465.
- [33] Vega-saenz de Miera EC, Rudy B, Sugimori M, et al. Molecular characterization of the sodium channel subunits expressed in mammalian cerebellar Purkinje cells. *Proc Natl Acad Sci U S A.* **1997**;94(13):7059–7064.
- [34] Raman IM, Sprunger LK, Meisler MH, et al. Altered subthreshold sodium currents and disrupted firing patterns in Purkinje neurons of *Scn8a* mutant mice. *Neuron.* **1997**;19(4):881–891.
- [35] Garcia KD, Sprunger LK, Meisler MH, et al. The sodium channel *Scn8a* is the major contributor to the postnatal developmental increase of sodium current density in spinal motoneurons. *J Neurosci.* **1998**;18(14):5234–5239.
- [36] Smith MR, Smith RD, Plummer NW, et al. Functional analysis of the mouse *Scn8a* sodium channel. *J Neurosci.* **1998**;18(16):6093–6102.
- [37] Boiko T, Rasband MN, Levinson SR, et al. Compact myelin dictates the differential targeting of two sodium channel isoforms in the same axon. *Neuron.* **2001**;30(1):91–104.

- [38] Caldwell JH, Schaller KL, Lasher RS, et al. *Sodium channel Na(v)1.6 is localized at nodes of ranvier, dendrites, and synapses*. Proc Natl Acad Sci U S A. 2000;97(10):5616–5620.
- [39] Tzoumaka E, Tischler AC, Sangameswaran L, et al. Differential distribution of the tetrodotoxin-sensitive rPN4/NaCh6/Scn8a sodium channel in the nervous system. J Neurosci Res. 2000;60(1):37–44.
- [40] Jenkins SM, Bennett V. Ankyrin-G coordinates assembly of the spectrin-based membrane skeleton, voltage-gated sodium channels, and L1 CAMs at Purkinje neuron initial segments. J Cell Biol. 2001;155(5):739–746.
- [41] Osorio N, Alcaraz G, Padilla F, et al. Differential targeting and functional specialization of sodium channels in cultured cerebellar granule cells. J Physiol. 2005;569(Pt 3):801–816.
- [42] Krzemien DM, Schaller KL, Levinson SR, et al. Immunolocalization of sodium channel isoform NaCh6 in the nervous system. J Comp Neurol. 2000;420(1):70–83.
- [43] Lorincz A, Nusser Z. Molecular identity of dendritic voltage-gated sodium channels. Science. 2010;328(5980):906–909.
- [44] Akin EJ, Solé L, Johnson B, et al. Single-molecule imaging of Nav1.6 on the surface of hippocampal neurons reveals somatic nanoclusters. Biophys J. 2016;111(6):1235–1247.
- [45] Golding NL, Spruston N. Dendritic sodium spikes are variable triggers of axonal action potentials in hippocampal CA1 pyramidal neurons. Neuron. 1998;21(5):1189–1200.
- [46] Meisler MH, Plummer NW, Burgess DL, et al. Allelic mutations of the sodium channel SCN8A reveal multiple cellular and physiological functions. Genetica. 2004;122(1):37–45.
- [47] Meisler MH, Kearney J, Escayg A, et al. Sodium channels and neurological disease: insights from Scn8a mutations in the mouse. Neuroscientist. 2001;7(2):136–145.
- [48] Levin SI, Meisler MH. Floxed allele for conditional inactivation of the voltage-gated sodium channel Scn8a (Nav1.6). Genesis. 2004;39(4):234–239.
- [49] Trudeau MM, Dalton JC, Day JW, et al. Heterozygosity for a protein truncation mutation of sodium channel SCN8A in a patient with cerebellar atrophy, ataxia, and mental retardation. J Med Genet. 2006;43(6):527–530.
- [50] Veeramah KR, O'Brien J, Meisler M, et al. De novo pathogenic SCN8A mutation identified by whole-genome sequencing of a family quartet affected by infantile epileptic encephalopathy and SUDEP. Am J Hum Genet. 2012;90(3):502–510.
- [51] Meisler MH, Helman G, Hammer MF, et al. SCN8A encephalopathy: research progress and prospects. Epilepsia. 2016;57(7):1027–1035.
- [52] Anand G, Collett-White F, Orsini A, et al. Autosomal dominant SCN8A mutation with an unusually mild phenotype. Eur J Paediatr Neurol. 2016;20(5):761–765.
- [53] Gardella E, Becker F, Møller RS, et al. Benign infantile seizures and paroxysmal dyskinesia caused by an SCN8A mutation. Ann Neurol. 2016;79(3):428–436.
- [54] Han JY, Jang JH, Lee IG, et al. A novel inherited mutation of SCN8A in a Korean family with benign familial infantile epilepsy using diagnostic exome sequencing. Ann Clin Lab Sci. 2017;47(6):747–753.
- [55] Gan J, Cai Q, Galer P, et al. Mapping the knowledge structure and trends of epilepsy genetics over the past decade: A co-word analysis based on medical subject headings terms. Medicine (Baltimore). 2019;98(32):e16782.
- [56] Akin EJ, Solé L, Dib-Hajj SD, et al. Preferential targeting of Nav1.6 voltage-gated Na<sup>+</sup> channels to the axon initial segment during development. PLoS One. 2015;10(4):e0124397.
- [57] Fleidervish IA, Lasser-Ross N, Gutnick MJ, et al. Na<sup>+</sup> imaging reveals little difference in action potential-evoked Na<sup>+</sup> influx between axon and soma. Nat Neurosci. 2010;13(7):852–860.
- [58] Kole MH, Stuart GJ. Is action potential threshold lowest in the axon? Nat Neurosci. 2008;11(11):1253–1255.
- [59] Huang CY, Rasband MN. Axon initial segments: structure, function, and disease. Ann N Y Acad Sci. 2018;1420(1):46–61.
- [60] Leterrier C. The axon initial segment: an updated viewpoint. J Neurosci. 2018;38(9):2135–2145.
- [61] Kordeli E, Lambert S, Bennett V. AnkyrinG. A new ankyrin gene with neural-specific isoforms localized at the axonal initial segment and node of Ranvier. J Biol Chem. 1995;270(5):2352–2359.
- [62] Jenkins PM, Kim N, Jones SL, et al. Giant ankyrin-G: A critical innovation in vertebrate evolution of fast and integrated neuronal signaling. Proc Natl Acad Sci U S A. 2015;112(4):957–964.
- [63] Kuijpers M, van de Willige D, Freal A, et al. Dynein regulator NDEL1 controls polarized cargo transport at the axon initial segment. Neuron. 2016;89(3):461–471.
- [64] Leterrier C, Vacher H, Fache M-P, et al. End-binding proteins EB3 and EB1 link microtubules to ankyrin G in the axon initial segment. Proc Natl Acad Sci U S A. 2011;108(21):8826–8831.
- [65] Kennedy SP, Warren SL, Forget BG, et al. Ankyrin binds to the 15th repetitive unit of erythroid and nonerythroid beta-spectrin. J Cell Biol. 1991;115(1):267–277.
- [66] Bennett V, Davis J, Fowler WE. Brain spectrin, a membrane-associated protein related in structure and function to erythrocyte spectrin. Nature. 1982;299(5879):126–131.
- [67] Xu K, Zhong G, Zhuang X. Actin, spectrin, and associated proteins form a periodic cytoskeletal structure in axons. Science. 2013;339(6118):452–456.

- [68] Leterrier C, Potier J, Caillol G, et al. Nanoscale architecture of the axon initial segment reveals an organized and Robust Scaffold. *Cell Rep.* 2015;13(12):2781–2793.
- [69] D'Este E, Kamin D, Göttfert F, et al. STED nanoscopy reveals the ubiquity of subcortical cytoskeleton periodicity in living neurons. *Cell Rep.* 2015;10(8):1246–1251.
- [70] Lemaillet G, Walker B, Lambert S. Identification of a conserved ankyrin-binding motif in the family of sodium channel alpha subunits. *J Biol Chem.* 2003;278(30):27333–27339.
- [71] Garrido JJ, Giraud P, Carlier E, et al. A targeting motif involved in sodium channel clustering at the axonal initial segment. *Science.* 2003;300(5628):2091–2094.
- [72] Pan Z, Kao T, Horvath Z, et al. A common ankyrin-G-based mechanism retains KCNQ and Nav channels at electrically active domains of the axon. *J Neurosci.* 2006;26(10):2599–2613.
- [73] Van Wart A, Trimmer JS, Matthews G. Polarized distribution of ion channels within microdomains of the axon initial segment. *J Comp Neurol.* 2007;500(2):339–352.
- [74] D'Este E, Kamin D, Balzarotti F, et al. Ultrastructural anatomy of nodes of Ranvier in the peripheral nervous system as revealed by STED microscopy. *Proc Natl Acad Sci U S A.* 2017;114(2):E191–E199.
- [75] Ogawa Y, Horresh I, Trimmer JS, et al. Postsynaptic density-93 clusters Kv1 channels at axon initial segments independently of Caspr2. *J Neurosci.* 2008;28(22):5731–5739.
- [76] Sarmiere PD, Weigle CM, Tamkun MM. The Kv2.1 K<sup>+</sup> channel targets to the axon initial segment of hippocampal and cortical neurons in culture and in situ. *BMC Neurosci.* 2008;9:112.
- [77] Bender KJ, Trussell LO. Axon initial segment Ca<sup>2+</sup> channels influence action potential generation and timing. *Neuron.* 2009;61(2):259–271.
- [78] Gasser A, Ho TS-Y, Cheng X, et al. An ankyrinG-binding motif is necessary and sufficient for targeting Nav1.6 sodium channels to axon initial segments and nodes of Ranvier. *J Neurosci.* 2012;32(21):7232–7243.
- [79] Shirahata E, Iwasaki H, Takagi M, et al. Ankyrin-G regulates inactivation gating of the neuronal sodium channel, Nav1.6. *J Neurophysiol.* 2006;96(3):1347–1357.
- [80] Mohler PJ, Rivolta I, Napolitano C, et al. Nav1.5 E1053K mutation causing Brugada syndrome blocks binding to ankyrin-G and expression of Nav1.5 on the surface of cardiomyocytes. *Proc Natl Acad Sci U S A.* 2004;101(50):17533–17538.
- [81] Brechet A, Fache M-P, Brachet A, et al. Protein kinase CK2 contributes to the organization of sodium channels in axonal membranes by regulating their interactions with ankyrin G. *J Cell Biol.* 2008;183(6):1101–1114.
- [82] Hien YE, Montersino A, Castets F, et al. CK2 accumulation at the axon initial segment depends on sodium channel Nav1. *FEBS Lett.* 2014;588(18):3403–3408.
- [83] Clatot J, Hoshi M, Wan X, et al. Voltage-gated sodium channels assemble and gate as dimers. *Nat Commun.* 2017;8(1):2077.
- [84] Schmidt JW, Catterall WA. Biosynthesis and processing of the alpha subunit of the voltage-sensitive sodium channel in rat brain neurons. *Cell.* 1986;46(3):437–444.
- [85] Catterall WA, Schmidt JW, Messner DJ, et al. Structure and biosynthesis of neuronal sodium channels. *Ann N Y Acad Sci.* 1986;479:186–203.
- [86] Leterrier C, Brachet A, Dargent B, et al. Determinants of voltage-gated sodium channel clustering in neurons. *Semin Cell Dev Biol.* 2011;22(2):171–177.
- [87] Winckler B, Forscher P, Mellman I. A diffusion barrier maintains distribution of membrane proteins in polarized neurons. *Nature.* 1999;397(6721):698–701.
- [88] Kobayashi T, Storrie B, Simons K, et al. A functional barrier to movement of lipids in polarized neurons. *Nature.* 1992;359(6396):647–650.
- [89] Brachet A, Leterrier C, Irondelle M, et al. Ankyrin G restricts ion channel diffusion at the axonal initial segment before the establishment of the diffusion barrier. *J Cell Biol.* 2010;191(2):383–395.
- [90] Nakada C, Ritchie K, Oba Y, et al. Accumulation of anchored proteins forms membrane diffusion barriers during neuronal polarization. *Nat Cell Biol.* 2003;5(7):626–632.
- [91] Garrido JJ, Fernandes F, Giraud P, et al. Identification of an axonal determinant in the C-terminus of the sodium channel Na(v)1.2. *Embo J.* 2001;20(21):5950–5961.
- [92] Fotia AB, Ekberg J, Adams DJ, et al. Regulation of neuronal voltage-gated sodium channels by the ubiquitin-protein ligases Nedd4 and Nedd4-2. *J Biol Chem.* 2004;279(28):28930–28935.
- [93] Fache MP, Moussif A, Fernandes F, et al. Endocytotic elimination and domain-selective tethering constitute a potential mechanism of protein segregation at the axonal initial segment. *J Cell Biol.* 2004;166(4):571–578.
- [94] Barry J, Gu Y, Jukkola P, et al. Ankyrin-G directly binds to kinesin-1 to transport voltage-gated Na<sup>+</sup> channels into axons. *Dev Cell.* 2014;28(2):117–131.
- [95] O'Brien JE, Sharkey LM, Vallianatos CN, et al. Interaction of voltage-gated sodium channel Nav1.6 (SCN8A) with microtubule-associated protein Map1b. *J Biol Chem.* 2012;287(22):18459–18466.
- [96] Villarroel-Campos D, Gonzalez-Billault C. The MAP1B case: an old MAP that is new again. *Dev Neurobiol.* 2014;74(10):953–971.
- [97] Cameron PL, Südhof TC, Jahn R, et al. Colocalization of synaptophysin with transferrin receptors: implications for synaptic vesicle biogenesis. *J Cell Biol.* 1991;115(1):151–164.
- [98] Song AH, Wang D, Chen G, et al. A selective filter for cytoplasmic transport at the axon initial segment. *Cell.* 2009;136(6):1148–1160.

- [99] Petersen JD, Kaech S, Banker G. Selective microtubule-based transport of dendritic membrane proteins arises in concert with axon specification. *J Neurosci.* 2014;34(12):4135–4147.
- [100] Watanabe K, Al-Bassam S, Miyazaki Y, et al. Networks of polarized actin filaments in the axon initial segment provide a mechanism for sorting axonal and dendritic proteins. *Cell Rep.* 2012;2(6):1546–1553.
- [101] Jones SL, Korobova F, Svitkina T. Axon initial segment cytoskeleton comprises a multiprotein submembranous coat containing sparse actin filaments. *J Cell Biol.* 2014;205(1):67–81.
- [102] Farias GG, Guardia CM, Britt DJ, et al. Sorting of dendritic and axonal vesicles at the pre-axonal exclusion zone. *Cell Rep.* 2015;13(6):1221–1232.
- [103] Gumy LF, Hoogenraad CC. Local mechanisms regulating selective cargo entry and long-range trafficking in axons. *Curr Opin Neurobiol.* 2018;51:23–28.
- [104] Gumy LF, Katrukha EA, Grigoriev I, et al. MAP2 defines a pre-axonal filtering zone to regulate kif1-versus kif5-dependent cargo transport in sensory neurons. *Neuron.* 2017;94(2):347–362 e7.
- [105] van Beuningen SFB, Will L, Harterink M, et al. TRIM46 controls neuronal polarity and axon specification by driving the formation of parallel microtubule arrays. *Neuron.* 2015;88(6):1208–1226.
- [106] Janssen AFJ, Tas RP, van Bergeijk P, et al. Myosin-V induces cargo immobilization and clustering at the axon initial segment. *Front Cell Neurosci.* 2017;11:260.
- [107] Setou M, Seog D-H, Tanaka Y, et al. Glutamate-receptor-interacting protein GRIP1 directly steers kinesin to dendrites. *Nature.* 2002;417(6884):83–87.
- [108] Rivera J, Chu P-J, Lewis TL, et al. The role of Kif5B in axonal localization of Kv1 K(+) channels. *Eur J Neurosci.* 2007;25(1):136–146.
- [109] Su YY, Ye M, Li L, et al. KIF5B promotes the forward transport and axonal function of the voltage-gated sodium channel Nav1.8. *J Neurosci.* 2013;33(45):17884–17896.
- [110] Zhang XL, Ding -H-H, Xu T, et al. Palmitoylation of delta-catenin promotes kinesin-mediated membrane trafficking of Nav1.6 in sensory neurons to promote neuropathic pain. *Sci Signal.* 2018;11(523):eaar4394.
- [111] Dash B, Han C, Waxman SG, et al. Nonmuscle myosin II isoforms interact with sodium channel alpha subunits. *Mol Pain.* 2018;14:1–12.
- [112] Grubb MS, Burrone J. Activity-dependent relocation of the axon initial segment fine-tunes neuronal excitability. *Nature.* 2010;465(7301):1070–1074.
- [113] Kuba H, Oichi Y, Ohmori H. Presynaptic activity regulates Na(+) channel distribution at the axon initial segment. *Nature.* 2010;465(7301):1075–1078.
- [114] Kuba H, Yamada R, Ishiguro G, et al. Redistribution of Kv1 and Kv7 enhances neuronal excitability during structural axon initial segment plasticity. *Nat Commun.* 2015;6:8815.
- [115] Evans MD, Sammons RP, Lebron S, et al. Calcineurin signaling mediates activity-dependent relocation of the axon initial segment. *J Neurosci.* 2013;33(16):6950–6963.
- [116] Evans MD, Tufo C, Dumitrescu AS, et al. Myosin II activity is required for structural plasticity at the axon initial segment. *Eur J Neurosci.* 2017;46(2):1751–1757.
- [117] Berger SL, Leo-Macias A, Yuen S, et al. Localized Myosin II activity regulates assembly and plasticity of the axon initial segment. *Neuron.* 2018;97(3):555–570.
- [118] Benned-Jensen T, Christensen RK, Denti F, et al. Live imaging of Kv7.2/7.3 cell surface dynamics at the axon initial segment: high steady-state stability and calpain-dependent excitotoxic downregulation revealed. *J Neurosci.* 2016;36(7):2261–2266.
- [119] Stoler O, Fleidervish IA. Functional implications of axon initial segment cytoskeletal disruption in stroke. *Acta Pharmacol Sin.* 2016;37(1):75–81.
- [120] Benusa SD, George NM, Sword BA, et al. Acute neuroinflammation induces AIS structural plasticity in a NOX2-dependent manner. *J Neuroinflammation.* 2017;14(1):116.
- [121] Schafer DP, Jha S, Liu F, et al. Disruption of the axon initial segment cytoskeleton is a new mechanism for neuronal injury. *J Neurosci.* 2009;29(42):13242–13254.
- [122] Hinman JD, Rasband MN, Carmichael ST. Remodeling of the axon initial segment after focal cortical and white matter stroke. *Stroke.* 2013;44(1):182–189.
- [123] Yermakov LM, Drouet DE, Griggs RB, et al. Type 2 diabetes leads to axon initial segment shortening in db/db mice. *Front Cell Neurosci.* 2018;12:146.
- [124] Buffington SA, Rasband MN. The axon initial segment in nervous system disease and injury. *Eur J Neurosci.* 2011;34(10):1609–1619.
- [125] Yamada R, Kuba H. Structural and functional plasticity at the axon initial segment. *Front Cell Neurosci.* 2016;10:250.
- [126] Ding Y, Chen T, Wang Q, et al. Axon initial segment plasticity accompanies enhanced excitation of visual cortical neurons in aged rats. *Neuroreport.* 2018;29(18):1537–1543.
- [127] Atapour N, Rosa MGP. Age-related plasticity of the axon initial segment of cortical pyramidal cells in marmoset monkeys. *Neurobiol Aging.* 2017;57:95–103.
- [128] Chand AN, Galliano E, Chesters RA, et al. A distinct subtype of dopaminergic interneuron displays inverted structural plasticity at the axon initial segment. *J Neurosci.* 2015;35(4):1573–1590.
- [129] Sohn PD, Huang CT-L, Yan R, et al. Pathogenic tau impairs axon initial segment plasticity and excitability homeostasis. *Neuron.* 2019;104:458–470.
- [130] Horschitz S, Matthäus F, Groß A, et al. Impact of preconditioning with retinoic acid during early development on morphological and functional characteristics of human induced pluripotent stem cell-derived neurons. *Stem Cell Res.* 2015;15(1):30–41.

- [131] Kuba H, Adachi R, Ohmori H. Activity-dependent and activity-independent development of the axon initial segment. *J Neurosci.* **2014**;34(9):3443–3453.
- [132] Duflocq A, Le Bras B, Bullier E, et al. Nav1.1 is predominantly expressed in nodes of Ranvier and axon initial segments. *Mol Cell Neurosci.* **2008**;39(2):180–192.
- [133] Hu W, Tian C, Li T, et al. Distinct contributions of Na(v)1.6 and Na(v)1.2 in action potential initiation and backpropagation. *Nat Neurosci.* **2009**;12(8):996–1002.
- [134] Bennett DL, Clark AJ, Huang J, et al. The role of voltage-gated sodium channels in pain signaling. *Physiol Rev.* **2019**;99(2):1079–1151.
- [135] Brouwer BA, Merkies ISJ, Gerrits MM, et al. Painful neuropathies: the emerging role of sodium channelopathies. *J Peripheral Nerv Syst.* **2014**;19(2):53–65.
- [136] Huang WY, Liu M, Yan SF, et al. Structure-based assessment of disease-related mutations in human voltage-gated sodium channels. *Protein Cell.* **2017**;8(6):401–438.
- [137] Li WJ, Yin L, Shen C, et al. SCN5A variants: association with cardiac disorders. *Front Physiol.* **2018**;9: 1372.
- [138] Parihar R, Ganesh S. The SCN1A gene variants and epileptic encephalopathies. *J Hum Genet.* **2013**;58(9):573–580.
- [139] Kaphzan H, Buffington SA, Jung JI, et al. Alterations in intrinsic membrane properties and the axon initial segment in a mouse model of angelman syndrome. *J Neurosci.* **2011**;31(48):17637–17648.
- [140] Sharkey LM, Cheng X, Drews V, et al. The ataxia3 mutation in the N-terminal cytoplasmic domain of sodium channel Na(v)1.6 disrupts intracellular trafficking. *J Neurosci.* **2009**;29(9):2733–2741.
- [141] de Kovel CG, Meisler MH, Brilstra EH, et al. Characterization of a de novo SCN8A mutation in a patient with epileptic encephalopathy. *Epilepsy Res.* **2014**;108(9):1511–1518.
- [142] Jones JM, Dionne L, Dell’Orco J, et al. Single amino acid deletion in transmembrane segment D4S6 of sodium channel Scn8a (Nav1.6) in a mouse mutant with a chronic movement disorder. *Neurobiol Dis.* **2016**;89:36–45.
- [143] Thompson CH, Porter JC, Kahlig KM, et al. Nontruncating SCN1A mutations associated with severe myoclonic epilepsy of infancy impair cell surface expression. *J Biol Chem.* **2012**;287(50):42001–42008.
- [144] Rusconi R, Scalmani P, Cassulini RR, et al. Modulatory proteins can rescue a trafficking defective epileptogenic Nav1.1 Na<sup>+</sup> channel mutant. *J Neurosci.* **2007**;27(41):11037–11046.
- [145] Dabby R, Sadeh M, Broitman Y, et al. Painful small fiber neuropathy with gastroparesis: A new phenotype with a novel mutation in the SCN10A gene. *J Clin Neurosci.* **2016**;26:84–88.
- [146] Kaluza L, Meents JE, Hampl M, et al. Loss-of-function of Nav1.8/D1639N linked to human pain can be rescued by lidocaine. *Pflugers Arch.* **2018**;470(12):1787–1801.
- [147] Keller DI, Rougier J, Kucera J, et al. Brugada syndrome and fever: Genetic and molecular characterization of patients carrying SCN5A mutations. *Cardiovasc Res.* **2005**;67(3):510–519.
- [148] Nunez L, Barana A, Amorós I, et al. p.D1690N Nav1.5 rescues p.G1748D mutation gating defects in a compound heterozygous Brugada syndrome patient. *Heart Rhythm.* **2013**;10(2):264–272.
- [149] Ruan Y, Denegri M, Liu N, et al. Trafficking defects and gating abnormalities of a novel SCN5A mutation question gene-specific therapy in long QT syndrome type 3. *Circ Res.* **2010**;106(8):1374–1383.
- [150] Leussis MP, Madison JM, Petryshen TL. Ankyrin 3: Genetic association with bipolar disorder and relevance to disease pathophysiology. *Biol Mood Anxiety Disord.* **2012**;2:18.
- [151] Schulze TG, Detera-Wadleigh SD, Akula N, et al. Two variants in Ankyrin 3 (ANK3) are independent genetic risk factors for bipolar disorder. *Mol Psychiatry.* **2009**;14(5):487–491.
- [152] Iqbal Z, Vandeweyer G, van der Voet M, et al. Homozygous and heterozygous disruptions of ANK3: At the crossroads of neurodevelopmental and psychiatric disorders. *Hum Mol Genet.* **2013**;22(10):1960–1970.
- [153] Yang R, Walder-Christensen KK, Lalani S, et al. Neurodevelopmental mutation of giant ankyrin-G disrupts a core mechanism for axon initial segment assembly. *Proc Natl Acad Sci U S A.* **2019**;116(39):19717–19726.